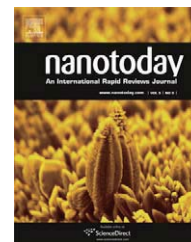


available at [www.sciencedirect.com](http://www.sciencedirect.com)



journal homepage: [www.elsevier.com/locate/nanotoday](http://www.elsevier.com/locate/nanotoday)



## REVIEW

# Designable 3D nanofabrication by femtosecond laser direct writing

Yong-Lai Zhang<sup>a</sup>, Qi-Dai Chen<sup>a</sup>, Hong Xia<sup>a</sup>, Hong-Bo Sun<sup>a,b,\*</sup>

<sup>a</sup> State Key Laboratory on Integrated Optoelectronics, College of Electronic Science and Engineering, Jilin University, Changchun 130012, China

<sup>b</sup> College of Physics, Jilin University, Changchun 130023, China

Received 6 June 2010; received in revised form 16 August 2010; accepted 25 August 2010

Available online 29 September 2010

### KEYWORDS

Femtosecond laser;  
Nanofabrication;  
Designable;  
Direct writing;  
Two-photon  
absorption

**Summary** Femtosecond laser direct writing (FsLDW) has been established as a nano-enabler to solve problems that are otherwise not possible in diversified scientific and industrial fields, because of its unique three-dimensional processing capability, arbitrary-shape designability, and high fabricating accuracy up to tens of nanometers, far beyond the optical diffraction limit. We briefly review the underlying mechanisms for achievement of the superhigh fabrication spatial resolution and surface smoothness, and then discuss the rule and photochemical strategies that are currently exploited for FsLDW. Finally, applications of the delicate nanoprototyping approach in microelectronics, micromechanics, microoptics and microfluidics are introduced. © 2010 Elsevier Ltd. All rights reserved.

## Introduction

Recent years have witnessed a rapid expansion of research on nanofabrication technologies towards tailoring artificial materials with desired nanostructures [1,2]. Bottom-up approaches, focusing on weak and reversible noncovalent interactions between molecules seek to have small, usually at molecular level, components built up into complex assemblies [3–8], while top-down approaches aim at creating nanoscale devices from bulky materials [9–12]. Although bottom-up approaches are feasible to produce two- and

three-dimensional (2D, 3D) structures at low cost, it still could not accommodate the increasing demand of structural complexity. Given that appropriate parallel processing strategies are discovered, a top-down technology may find broader usage in manufacturing structurally complex and functionally advanced devices. For example, semiconductor, metal and polymer planar patterns have been readily created by digital way for use in integrated circuits, and optoelectronic applications by (i) lithography, which makes use of ultraviolet (UV) light, X-ray or focused electron beam to expose mask-defined patterns [13–17]; (ii) nanoimprint or inject printing, which creates patterns either by mechanical deformation of imprint resist or by propelling variably sized droplets of liquid material (ink) or powder onto a substrate [18–20]. In spite of the nanometric resolution, the available geometry directly achieved by these means is commonly limited to 2D patterns. A nanoprocessing technology that simultaneously possesses the merit of

\* Corresponding author at: State Key Laboratory on Integrated Optoelectronics, College of Electronic Science and Engineering, Jilin University, 2699 Qianjin Street, Gaixin, Changchun 130012, Jilin, China. Tel.: +86 431 85168281; fax: +86 431 85168281.

E-mail address: [hbsun@jlu.edu.cn](mailto:hbsun@jlu.edu.cn) (H.-B. Sun).

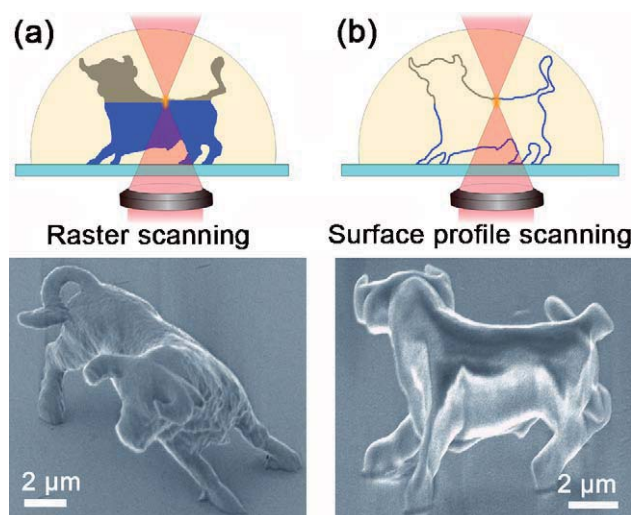


**Figure 1** Examples of micro-nanofabrication with sub-diffraction-limit resolution. A titanium sapphire laser operating in model-lock at 76 MHz and 780 nm with a 150-fs pulse width was used as an exposure source. The laser was focused by an objective lens of high numerical aperture ( $\sim 1.4$ ). (a) Scheme and SEM images of bull sculpture fabricated by raster scanning; the process took 180 min. (b) Bull sculpture fabricated by surface-profile scanning and subsequent solidification under a mercury lamp; the process took 13 min. Reproduced with permission from [30]. ©2001 Nature Publishing Group.

3D architecting like supramolecular self-assembly and the highly designability like lithography and printings, is therefore highly desired.

Femtosecond laser direct writing (FsLDW) has been recently recognized as a promising candidate to reach the above end [21–30]. It is performed by scanning a tightly focused laser beam according to designed patterns from the bottom slice to the upside slice until the entire 3D structure is achieved. Shown in Fig. 1 are the sculptures of microbulls as the example of FsLDW [30]. Because of the extremely large transient power density, e.g.,  $10^{13}$  W/ $\mu\text{m}^2$  for a mediate irradiation, photons are absorbed in a nonlinear manner (two- or multi-photon absorption, TPA and MPA, is mostly used) in a volume much smaller than the cubic wavelength,  $\lambda^3$  [31]. The high spatial resolution of FsLDW, till tens of nanometers, much beyond the optical diffraction limit, is therefore achieved [32]. In order to take full use of the nonlinear light–matter interactions, light source with near-infrared wavelength is generally chosen. In this case, the laser light deeply penetrates into a bulk without absorptive power loss, making it possible to tailor materials from inside, i.e., the 3D processing capability. The 3D patterns are preprogrammed by computer, as is the origin of high designability of FsLDW. Since various materials including organic molecules, dielectrics, metal and semiconductors [33,34] are reactive under femtosecond laser irradiation, FsLDW also distinguishes itself from other currently available nanoprocessing methods as a universal tool only if a proper photochemical strategy is determined.

In this review, we first introduce how the fabrication accuracy has been dramatically improved to nanomet-

ric order so that FsLDW appears as a new member in nanofabrication field; then FsLDW devicing mechanisms based on photopolymerization, photoisomerization, photoreduction and other novel laser induced photochemical transformation processes were summarized. Finally, we shall present a brief introduction and future perspective of their applications in the various scientific and industrial fields such as microoptics, micromachines, microelectronics, and microfluidic chips.

### Nanometric fabrication accuracy

The issue of fabrication resolution is of fundamental concern for a micro-nanoprocessing tool. In nanoimprinting and inject printing, mechanical force exerted by the side wall of molds or the nozzle functions for spatial confinement of materials to tiny scale, while for various lithographies, the spatial resolution improvement should be ascribed to continuous efforts towards usage of shorter wavelength from ultraviolet (UV,  $\lambda \sim 100$  nm for excimer lasers), extreme ultraviolet (EUV,  $\lambda < 10$  nm), X-ray ( $\lambda < 1$  nm), to electron beams ( $\lambda < 0.1$  nm) so that smaller beam–matter interaction volume is defined [14,15]. The nature of two- or multi-photon absorption excludes the possibility to pursue higher resolution by the same technical avenue since most organic molecules are absorptive in the visible to UV wavelength range, for which alternative principles have to be adopted.

The first factor that contributes to the improvement of FsLDW resolution is nonlinear optical effect. For linear exposure such as lithography, materials respond to light excitation to the first order effect, while for two- and multi-photon absorption, the response is restricted to two and high orders. The square light intensity distribution is spatially narrower than that of linear one [32], resulting in a reduction of light–matter interactive volume, and therefore, the improvement of fabrication resolution. Here, we have to mention that it is not practical to pursue better resolution by purposely employing higher order effects, for which longer wavelengths have to be utilized. This would counteract the nonlinearity-induced resolution improvement.

In addition to optical nonlinearity, further improvement of the spatial resolution appeals to thresholding effect, also called chemical nonlinear effect, which functions simultaneously [32]. Take two-photon induced polymerization of resins (see sessions below for details) as an example, photogenerated radicals are spatially distributed obeying the square law of the light intensity function. The rate of photopolymerization of monomers is therefore expected to follow the same distribution. However, due to the existence of the radical quenchers like dissolved oxygen molecules, radicals survive and initiate polymerization only at the region with higher light intensity, and thus the threshold is formed. Since the light intensity relative to the threshold is continuously adjustable by exposure duration or laser pulse intensity, the size of volume elements [35–40], or voxels, used as the basic building block of targeted structures and a reflection of the fabrication spatial resolution, was tuned much smaller than that defined by the diffraction limit. The lateral size of voxels in Fig. 2a is around 120 nm. When alternative radical quenchers were chosen, it was reduced to less than 100 nm. Since the thresholding mechanism has been found exten-

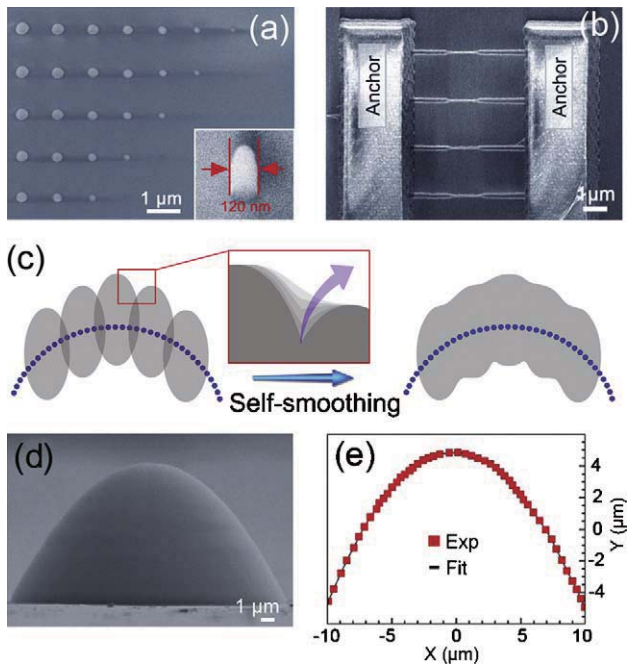


**Figure 2** (a) Illustration of the achievement of sub-diffraction-limit (SDL) fabrication accuracy. A SEM image of voxels obtained in different TPA exposure conditions; (b) SEM image of suspended array of nanowires. The exposure duration of the ended and the central segments is, under a laser pulse energy of 75 pJ at the focal spot, 8 and 2 ms, respectively; (c) illustrative model to show the voxels overlapping induced high resolution. A much smoother surface could be obtained after developing due to a self-smoothing process; (d) SEM image of a parabolic microlens; (e) the measured profile (the square symbol) and the theoretical curves (the line). Reproduced with permission from [32,41,44]. ©2002 American Institute of Physics, 2009 Optical Society of America, 2009 IEEE.

sively existing in various materials, it is the most important factor that contributes to spatial resolution improvement in FsLDW. For the particular case of photopolymerization of resins, the unpolymerized monomer or photoinitiator molecules or molecular segments are removable from the polymer network. If the written feature is sufficiently small such as suspended thin fibers, the diameter can be further reduced, e.g., reproducible 65 nm (Fig. 2b) [41] and in some occasions 25 nm [42]. This effect is called materials nonlinearity.

The combinative action of optical, chemical and material nonlinearities makes it possible to achieve reproducible fabrication resolution of tens of nanometers, at a level of  $\lambda/10$  to  $\lambda/50$ , much smaller than the optical diffraction limit. Theoretically, voxels may be further reduced in size only if laser pulse energy is regulated closer to but still above the threshold level. However, it is tough to experimentally confirm since individual voxels resulted from low exposure are mechanically too weak to resist rinsing for removal of unexposed portion and survive electron beam exposure.

The FsLDW fabrication accuracy is generally determined by the smallest achievable voxel sizes, but higher precision has been achieved in practical model prototyping [43], as was ascribed to the unique merits of the technol-

ogy. First, unlike self-assembling of colloidal nanoparticles, which turns to close package of rigid spheres, complicated structures are built from voxels that can overlap with each other in the case of FsLDW (Fig. 2c). Desired center-to-center distance is readily chosen, meaning the possibility of dimension definition to any value larger than voxel itself with precision much beyond the restriction of voxel size. The higher precision was technically guaranteed by the following factors: (i) high reproducibility of the shape and size of voxels [35–38]. The laser pulse energy instability, generally less than 5%, leads to fluctuation of voxels size less than 5 nm; and (ii) high positioning accuracy of voxels due to the usage of piezo moving stage with motion accuracy better than 1 nm or mirror steering with accuracy of several nanometers. The overall spatial resolution in FsLDW in common shape design reaches as good as sub-20 nm [44].

In addition to the accuracy of dimension definition, another important factor that may affect device functions is surface quality, particularly for optical components [44,45]. In two-photon induced photopolymerization of resins, surface quality better than that mentioned above has been acquired. For example, when the scanning pitch is reduced to around 100 nm for voxels of 100 nm lateral diameter, the surface protrusion was stabilized at 10 nm level [43]. Shown in Fig. 2d is a FsLDW created curved surface, the side view SEM image of an ellipsoid-shaped aspheric microlens. The surface roughness is estimated at 2.5 nm, and the overall deviation of the surface from design was measured to be 17.3 nm [44]. Such a high surface smoothness cannot be interpreted solely by voxels overlapping. Underlying mechanisms have to be explored. By a careful study one may find that the corner formed at the boundary of two neighboring voxels is sharp (Fig. 2c), where the surface Gibbs free energy is expected to be smaller than that at the voxel tip end. The unpolymerized resin trapped there is thus difficult to remove in the rinsing process. Furthermore, the locally rugged surface tends to be straightened due to surface tension when the surface starts to expose to air. The local surface reforming due to the surface tension, also called self-smoothing effect, can significantly improve the surface quality [43].

## Photochemical schemes for FsLDW

Because of the high transient power, femtosecond laser can excite various materials and induce irreversible photochemical or photophysical reactions. Only if an appropriate devising strategy is discovered, the process may be utilized for micro-nanofabrication. Exploration to novel materials, novel photochemical mechanisms and novel photo-optical technologies to satisfy the increasing demand in micro-nanodevices constitutes an important driving force for the technology progress. Significant progress has been achieved with the efforts made by the experts all over the world in recent years. As shown in Table 1, the fabrication accuracy of nanostructures created *via* FsLDW has reached sub-20 nm. The photochemical scheme for FsLDW ranges from photopolymerization to photoreduction, photoisomerization and so on (Table 1). Shown in Fig. 3a is a representative FsLDW system, which consists functionally of four parts: laser source and beam direction system (the left column), beam steering and motion stage (the right column), com-

**Table 1** Progress of FSLDW photochemical schemes during the last five years (2006–2010).

Photochemical scheme	Typical works and groups	Strategy	Achievement	Applications	Ref.
Photopolymerization	100 nm resolution (K.S. Lee et al.)	Addition of radical quenchers	High efficiency	Microstructures	[27]
	40 nm feature size (J.T. Fourkas et al.)	Use of activation beam	High resolution	Microdevices	[24]
	25 nm resolution (X.M. Duan et al.)	Scanning speed manipulation	High resolution	Micromachines, P-MEMS <sup>b</sup>	[42]
	20 nm resolution (H.B. Sun et al.)	Self-smoothing effect	High resolution	Microoptics	[43]
Doped photopolymerization	Optical data storage (M. Gu et al.)	Doping with gold nanorods	High data density	Data storage	[33]
	Magnetic micromachines (H.B. Sun et al.)	Photopolymerizable ferrofluids	Remote control	Micromachines	[53, 54]
Photoreduction	Luminescent microstructures (X.M. Duan et al.)	In situ synthesis	Luminescent function	Microsensors	[34]
	Metallic structure in polymer (S. Maruo et al.)	Photoreduction in polymer matrix	Metallic microstructure	LoC <sup>a</sup>	[81]
	3D metallic microstructures (X.M. Duan et al.)	Surfactants assistance	3D metallic microstructure	IC <sup>c</sup>	[83]
	Conductive 3D Ag nanowiring (H.B. Sun et al.)	Stable silver precursor	Nonplanar nanowiring	IC	[85]
Photoprecipitation	3D TiO <sub>2</sub> PhCs <sup>d</sup> (M.S.M. Saifullah et al.)	Photosensitive sol–gel	Oxides microstructure	Microoptics	[73]
	SnO <sub>2</sub> microsensor (H.B. Sun et al.)	Photo-induced solubility change	Flexible integration	Microsensor	[74]
Other routes	Photoisomerization (H.B. Sun et al.)	Solubility change for fabrication	All PPV <sup>e</sup> microstructures	Microdevices	[72]
	Photoreduction of GO <sup>e</sup> (H.B. Sun et al.)	Laser induced deoxidation	Patterning of graphene	IC	[51]
	Protein 3D topography (J.B. Shear et al.)	Photocrosslink of protein	3D bio-microstructures	Cell biology	[68–70]

<sup>a</sup> Lab-on-a-chip system.

<sup>b</sup> Polymer microelectromechanical system.

<sup>c</sup> Integrated circuits.

<sup>d</sup> Photonic crystals.

<sup>e</sup> Poly(p-phenylene vinylene).

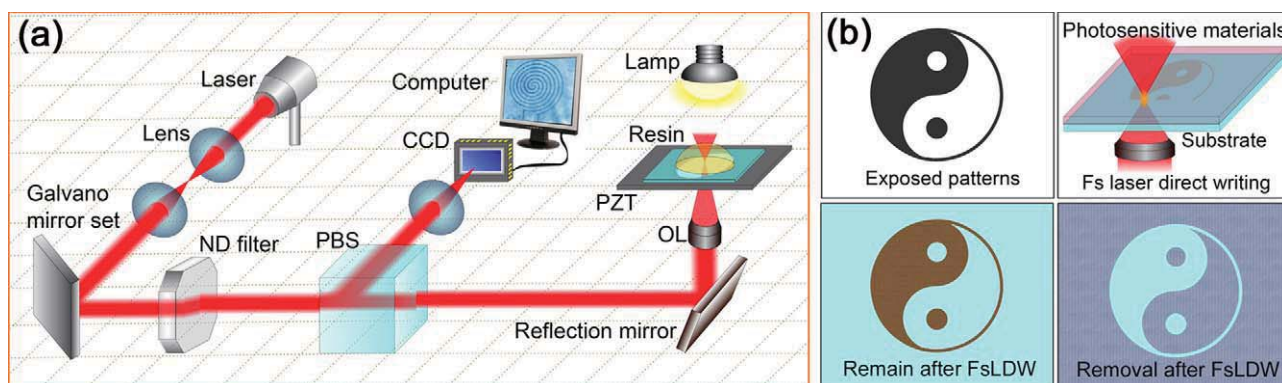


**Figure 3** (a) Schematic femtosecond laser direct writing system. The use of femtosecond laser and tightly focusing light by a high NA lens (1.4, oil immersion used here) is critical to launch the nanofabrication process. The output stability of laser pulse energy and the accuracy of focal spot/sample scanning are the most important factors that guarantee a high precision fabrication. The imaging system using a CCD camera is useful both for optical adjustment and for in situ fabrication monitoring. PBS: polarization beam splitter; OL: objective lens; PZT: piezoelectric transducer; (b) scheme of photosensitive materials that are used for femtosecond laser direct writing according to preprogrammed patterns. Laser induced solidification would result in removal of the unexposed region, whereas laser induced dissolution would lead to removal of the exposed region.

puter graphic generation and control system (not shown), and in situ monitoring system (the middle column). Under the computer control, materials placed on the motion stage were irradiated by the focused femtosecond laser, locally inducing material properties variation with sufficient contrast to unexposed background, among which the most important is the change of solubility to a certain solvents. Either the irradiated or unexposed portions are to be removed by the rinsing process (Fig. 3b). The former examples include two-photon FsLDW of positive-tone photoresist [46,47], and transparent solids like glasses [48], in which irradiated volume becomes photochemically more active due to bond breaking and is therefore liable to be removed [49]. In the latter case, the femtosecond laser irradiation enhances intermolecular interactions, by covalent bond formation in photopolymerization of resins or by electrostatic and van der Waals' forces in photoreduction of metal ions and isomerization. The rinsing process is not always necessary for device functions, for example, waveguide and grating formation [50] and graphene microelectronic circuits drawing from photoreduction of graphene oxide film [51], where the background constitutes an essential part due to their optical (low index of refraction), electrical (insulation) and mechanical (supporting) functions. In the following part, we will introduce these established mechanisms to trigger more studies along this line.

### Two-photon-induced photopolymerization

FsLDW based on two-photon induced photopolymerization of resin is a well established approach for prototyping various micro-nanostructures. The fundamental ingredients of resins include: photoinitiators that are used for radicals generation after excited, monomers or oligomers that act as the main skeleton of micro-nanostructures, and cross-linkers that ensure an insolubility in the developing solvents. For practically used photoresists, more components are included, for example, multiple photoinitiators, photosen-

sitizers and other functional molecules or even inorganic doping agents [52–54]. Upon light excitation, an initiator molecule absorbs a UV photon, or simultaneously absorbs two near-infrared (NIR) photons, being excited into radicals. The radicals react with monomers, producing monomer radicals, which were combined with new monomers. Thus, the monomer radicals expand in a chain reaction, until two radicals meet with each other. Photopolymerization ends up with the exhaustion of radicals or other ingredients. Oligomer constitutes the backbone of the polymer network, determining the physical, chemical, and mechanical properties of the solidified resin. Besides the role as a reactive precursory, monomers exist also for diluting resins so that the polymer is easy to handle. For 3D micro-nanolithography, a suitable viscosity is particularly important due to the opposite requirements in different steps of processing: a high viscosity is needed for preventing early produced voxels from floating and kept temporary part where it was created; while a low viscosity facilitates removing un-solidified resin from channel intervals. A trade off of the resin viscosity has to be made considering features of each targeted structures. Shown in Fig. 4 are two-photon photopolymerized 3D structures. The micro-thinker (Fig. 4a) [55], micro-gate (Fig. 4b) [56], and microfluidic channel require high mechanical strength for self-supporting, while relatively high-density channels exist in the microgears and micro-chains [57], as well as the photonic crystals (PhCs) [58,59], challenge the completeness of resin removal. The low mechanical strength in the above structures is sometimes problematic if devices of larger scale are pursued. It is expected to solve by novel route of synthesis of monomers or oligomers of high-density unsaturated bonds that are useful for photopolymerization and cross-linking.

The unique high precision 3D prototyping capability of two-photon photopolymerization has been fully approved. However, its shortcoming for industrial use is also apparent, i.e., the relatively low fabrication efficiency caused by the nature of single beam scanning. Although the same problem has been encountered in electron beam lithogra-

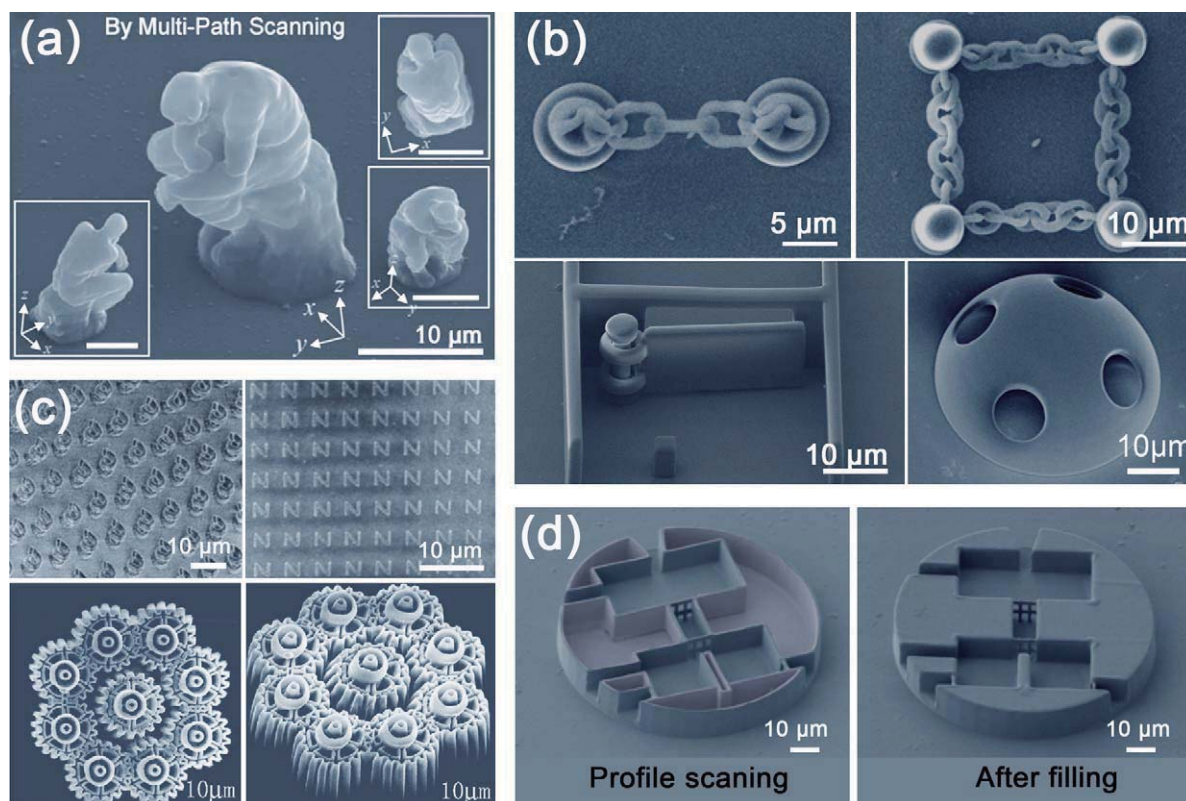


**Figure 4** Examples of micro-nanostructures created with femtosecond laser induced photopolymerization. (a) SEM images of micro-Thinker fabricated by double-scanning path. The insets are the same micro-Thinker with various view angles; (b) SEM images of movable devices (micro-chain structures) and nanoshell structure created with FsLDW; (c) SEM images of examples of two- and three-dimensional fabrication with the parallel processing technique: the microletter array of 'N' was fabricated with 28 exposure points in two-dimension, in which totally 227 structures were fabricated using the relay lens of 150-mm-focal length; the example of 3D fabrication, where the self-standing micro-spring array was fabricated with the relay lens of 80-mm-focal length. The bottom is SEM images of top and side views of assembled microgear set. (d) A conceptual microfluidic device fabricated by FsLDW of SU-8. SEM images of the 3D microfluidic systems with 100  $\mu\text{m}$  diameter disk and 15  $\mu\text{m}$  height. The internal portion of the background volume is solidified by additional ultraviolet exposure. Reproduced with permission from [55,56,60,61]. ©2005, 2007 American Institute of Physics; ©2009 The Royal Society of Chemistry.

phy (EBL) and focused ion beam (FIB), it is difficult to solve there since no proper parallel processing mechanism as done in photolithography may be found. Femtosecond laser as an electromagnetic wave, different from the particle beams, is likely split by diverse optical techniques like diffraction and wavefront cutting. Some of the current authors first split one incident light by a microlens array and then focused multiple beams to the resin [60], whereby more than 200 micro-objects like letter 'N' and micro-coils were produced in one-run scanning ( $\sim 5$  min, Fig. 5c). Diffraction beam splitter [61] was also adopted to divide an incident beam, by which 9 microgears with diameters of 15  $\mu\text{m}$  were simultaneously produced. The strategy of beam splitting for parallel processing is a promising avenue towards low cost 3D FsLDW batch production. Other technologies towards fabrication efficiency improvement have been also tried. For example, defining only the surface layer of particular structures like the shell of a microfluidic device by pinpoint two-photon polymerization [56], while solidifying their inner supporting portion by UV exposure reduces the overall fabrication time by up to 90% (Fig. 4d). The issue of low fabrication efficiency should be ultimately solved by joint efforts from chemical

(e.g., photopolymers of smaller threshold of photopolymerization), optical (e.g., exploration of the possibility of using more parallel beams while maintain an identical power, intensity profile and sometimes polarizations of beamlets) and electronic (faster data conversion and transportation speed and faster response of optical components) efforts.

Besides the technical breakthroughs, the development of FsLDW may also depend on design and synthesis of photosensitive molecules considering the following points. (i) The need of parallel processing. Parts number from parallel processing is not limited by the available beam number, which actually can be infinite, but is restricted by the laser pulse energy of each beamlets after beam splitting, which should be large enough to trigger two-photon reactions. It has been found that  $\pi$ -conjugated systems possess high two-photon absorption cross-sections, e.g., initiator molecules with phenylethenyl [62], fluorenyl [63], or polyenyl constructs [64]. In these molecules, electron-donating (D) and/or electron-withdrawing (A) moieties were separated by a conjugated  $\pi$ -electron system, i.e., A- $\pi$ -A, D- $\pi$ -D, D- $\pi$ -A- $\pi$ -D and A- $\pi$ -D- $\pi$ -A [65,66]. These chromophores function on the basis that symmetric charge

transfers from the ends of a conjugated system to the middle or vice versa. Photoinitiators with two-photon absorption cross-sections as high as  $\sim 1250 \times 10^{-50} \text{ cm}^4 \text{ s photon}^{-1}$  were synthesized according to this concept and were successfully utilized for FSLDW [23]. Not only initiators for negative-tone resins were widely studied, novel two-photon-activatable photoacid generators (PAG), based on a *bis*[(diarylamino)styryl] benzene core with covalently attached sulfonium moieties (BSB-S<sub>2</sub>), have also been synthesized for 3D fabrication of acid sensitive positive-tone resists. The PAG of BSB-S<sub>2</sub> has both a large two-photon absorption cross-section and a high quantum yield for the photochemical generation of acid, which is crucial in activation of various reactions, such as the ring opening of epoxides and cleavage reactions [46]. Using this photoinitiator and a positive-tone photoresist, interconnected micro-channels were successfully prepared using very low irradiation power owing to its high two-photon sensitivity of this material system. The positive-tone resin is promisingly useful for fabrication structures abundant of channels like microfluidic devices. (ii) The requirement of device functionalization. So far, resins are sufficient to define geometrical shape of various devices and provide mechanical sustentation. In order to further induce desired optical, electronic, magnetic, and mechanical tuning performance into devices, photopolymerizable functional molecules design and host-guest doping, both for FSLDW have been attempted. For polymer microelectromechanical system (P-MEMS), the optical functions such as transparency and light emission [44], and mechanical movements [53,54] are relatively easier to carry out. How to achieve electronic conductivity is a kind of nodus of P-MEMS. Efforts have been paid on electroless plating, dope of metal nanoparticles and carbon nanotubes, which may give promising solutions in the near future. Also worthy to mention is complex structure fabrication using biomaterials such as proteins (Fig. 5a–c) [67–71]. The 3D bio-coordinates are sensitive to chemical environment, and therefore, a novel pH response mechanical manipulation of the protein 3D topography was achieved as bacterial cages towards cell biology use (Fig. 5c) [68]. Considering their biocompatibility, the bio-micro-nanostructures may find use in, for example, cells growth steering in cages towards tissue regeneration, in deep insight into cell differentiation in lab-on-a-chip system, and micro-robots for drug delivery, disease diagnosis and treatment [67]. It is worthy to mention that the high fabrication quality as represented by the 20-nm spatial resolution and 2.5 nm surface roughness have so far been achievable only in several most studied and widely utilized material systems. There is much room left to material scientists to improve the polymer compositions by guest-host doping or by molecular design for diversified functional device requirements.

### Two-photon-induced precipitation

A problem in guest-host doping, the most widely used approach for fabrication of functional devices, is the limited loading percentage of effective components, generally to several percent in mass, resulting in high threshold and high external stimuli for device operation. It is reasonable to explore alternative strategies other than

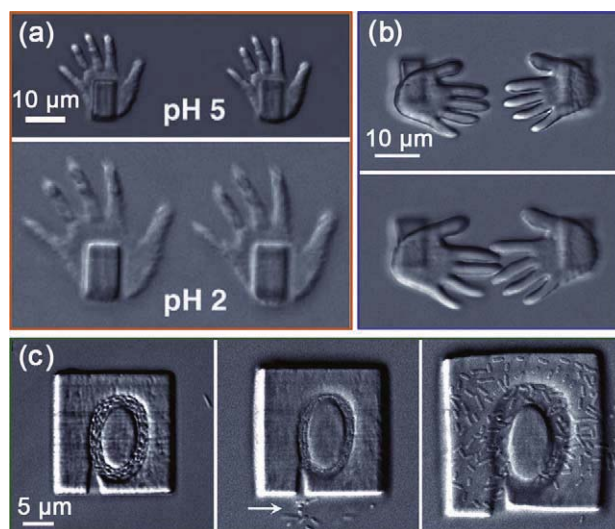


**Figure 5** Micro-nanofabrication of photoresponsive protein hydrogels. (a) BSA microhands mounted on BSA pedestals  $\sim 4 \mu\text{m}$  from the coverslip surface (upper) undergo reversible swelling after a decrease in bath pH from 5 to 2 (lower); (b) BSA hydrogel microstructures with high resolution and arbitrary topography. Interdigitation of middle fingers achieved when the bath solution is changed; (c) dynamic microchambers for cell culture. Abrupt change in bath pH (7–12.2) causes temporary compression of the internal chamber. Reproduced with permission from [68]. ©2008 by The National Academy of Sciences of the USA.

photopolymerization, which are expected to create functional micro-nanodevices with high concentration of active ingredients as the basic building block through femtosecond laser fabrication. As mentioned above, FSLDW is not limited to photopolymerizable materials. In fact, any photochemical reaction would be adopted for designable micro-nanostructuring only if a significant phase transformation occurs, for example precipitation, after two- or multi-photon absorption.

Photoisomerization is a photo-initiated structural change between *trans*- and *cis*-forms of isomers [72]. It is already well established that the *trans*-to-*cis* or *cis*-to-*trans* isomerization could be photostimulated by TPA. The alteration of geometric structures renders significant change in solubility, which contributes the feasibility of laser processing. As a typical example, Xia et al. [72] reported a fabrication of micro-nanostructures based on two-photon absorption initiated photoisomerization of poly(*p*-phenylene vinylene) (PPV) derivative (Fig. 6a). Upon the near-infrared femtosecond laser irradiation, a *cis*-form DPO-PPV underwent molecular conformational change into *trans*-form DPO-PPV with rotational motions of the double bonds. The *cis*-form is readily soluble in common organic solvents because of the twisting configuration of the *cis*-vinylene segments, while the solubility of *trans*-form becomes worse due to the stronger intermolecular attractions arising from the more-coplanar molecule conformation. Taking advantage of the significantly reduced solubility of the *trans* DPO-PPV, micro-nanostructures consisting of nearly 100% *trans* DPO-PPV are fabricated by pinpoint laser writing in *cis* DPO-PPV precursor (Fig. 6b and c). As an important electrolumines-

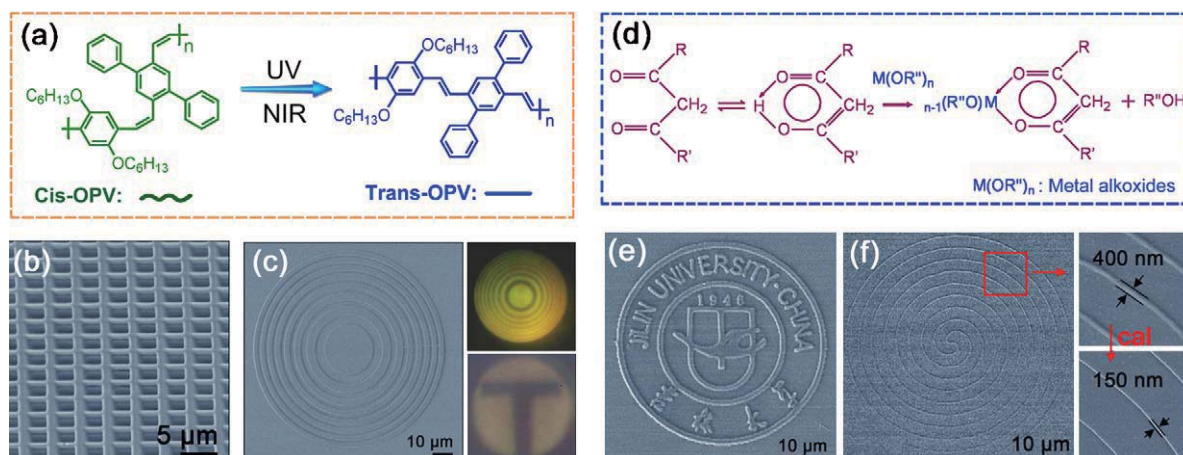


**Figure 6** Examples of micro-nanostructures created with femtosecond induced solubility debasement. (a) The molecular configuration conversion of DPO-PPV from *cis*-form twisting structure to *trans*-form rigid coplanar structure under UV or near IR light; (b) SEM image of an as-created 3D microstructures; (c) Fresnel zone plate of DPO-PPV fabricated by the same way. The plate exhibits true color of *trans* DPO-PPV under illumination by a Xenon lamp and a letter “T” was imaged by the DPO-PPV Fresnel plate; (d) synthetic equation of photosensitive chelate metal oxides sol that could be used for laser processing; (e) SEM image of the badge of Jilin University as an example of complex micro-nanostructures created with  $SnO_2$  sol. (f) After thermal treatments, crystalline  $SnO_2$  nanostructures with higher resolution could be obtained due to the removal of organic components. Reproduced with permission from [72,74]. ©2009 American Institute of Physics, 2010 Optical Society of America.

cent material, micro-nanostructured PPV and its derivatives fabricated through the novel two-photon induced photoisomerization would exhibit promising prospect in organic light-emitting devices. To this end, novel device structures are to be invented, where appropriate electrodes design required by the low mobility of carriers in organic semiconductors is the first issue to address.

Micro-nanostructured inorganic semiconductors exhibit great potential in the applications of electrical, sensitive and optical devices [73]. Generally, nanostructured inorganic materials such as metal oxides could be prepared by conventional “bottom-up” and “top-down” approaches, whereas these techniques make rigorous demands on the substrates flatness, and thus suffer from poor compatibility for integration with other microdevices. If the 2D or 3D semiconductor oxides could be created in a designed manner on any desired substrates, significant contributions would be made for integration and miniaturization of microdevices [74]. In order to make the inorganic materials suitable for FsLDW, novel sol–gel-based metal chelates have been successfully developed as photosensitive inorganic source for laser processing [73–75]. As the first example, photosensitive spincoated  $TiO_2$  resist was prepared by chemical modification of titanium *n*-butoxides,  $(Ti(OBu^n)_4)$ , with benzoylacetone, BzAc. The metal alkoxides are very reactive compounds because of the presence of electronegative alkoxy groups which make the metal atoms highly prone to nucleophilic attack. Two-photon excitation, similar to the cases of UV and electron beam exposures, resulted in the breakdown of the C–C and C–O bonds in the chelate ring, which in turn reduced their solubility in alcohols and acidic solutions. Packing exposure-induced atoms or clusters according to laser scanning traces led to desired 2D or 3D patterns. Similarly,  $SnO_2$  fine patterns have been produced in the same way (Fig. 6d). Because of the particular material properties, the  $TiO_2$  3D patterns have utilized as

photonic crystals considering its high optical transparency and high index of refraction, while  $SnO_2$  has been directly patterned into a microsensors. The merits of the technology as mentioned earlier lie in the possibility of (a) high percentage loading of effective composition up to 100%, as compared with the several percentage in matrix doping, and (b) adding needed elements in ready circuits and on nonplanar substrates. The patterned structures need post-processing, typically annealing, to remove organic residue, which generally leads to significant distortion of written structures. The phenomenon has been positively utilized as a strategy to reduce the feature size of devices (Fig. 6e and f). In most cases, particular care has been taken for high-fidelity fabrication.

### Two-photon-induced photoreduction of metal ions

Metal structures with nanoscale feature have received intensive attention due to their unique properties in the fields of chemistry [76], plasmonics [77], microelectronics [78] and bioscience [79]. Therefore, efforts have been devoted to fabrication of metal nanostructures through various nanofabricative routes. However, up to date, it is still a challenging task to obtain 3D structures with nanoscale spatial resolution. For metal nanofabrication *via* FsLDW, photoreduction reactions were considered as preferred processes to generate metal building blocks. However, photoreduction usually undergoes the process of isolated metal nanoparticles growing up and aggregation which is uncontrollable, and therefore, usually results in poor metallic microstructures. In order to avoid this unwanted effect, various novel routes were developed. For example, 3D metallic microstructures were successfully created in the polymers matrix containing homogeneously doped metal ion [80–82]. Due to the effective support of polymer matrix, continuous

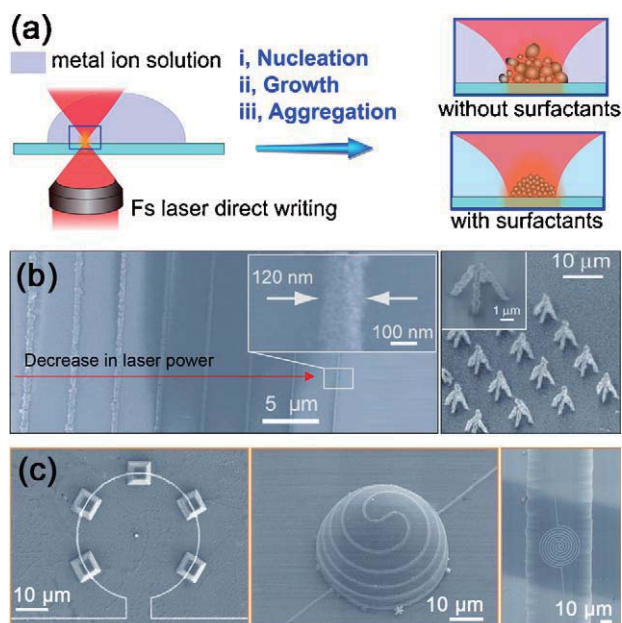


**Figure 7** Examples of micro-nanostructures created with femtosecond induced photoreduction. (a) Schematic illustration for fabrication of metallic micro-nanostructures by FSLDW induced photoreduction of metal ions solution. Surfactants were used as metal particles growth inhibitor for achieving high resolution; (b) SEM image of silver stripe patterns formed using different laser powers and a linear scanning speed of  $6 \text{ mm s}^{-1}$  and the free-standing silver pillar on the cover slip, made using a laser power of  $1.14 \text{ mW}$  and a linear scanning speed of  $\text{mm s}^{-1}$ ; (c) FSLDW for silver nanowiring on 3D substrates (from left: frustum of pyramids, hemisphere and microfluidic channel). Reproduced with permission from [83,85]. ©2009, 2010 Wiley–VCH.

microstructures could be retained after developing. However, the resolution of these 3D metallic structures was still low owing to the presence of unreacted polymers. Typically, the major problem that restricts spatial resolution of metal micro-nanostructure fabricated *via* FSLDW is the uncontrollable growth and aggregation of metal nanoparticles during photoreduction process. If the thermal reduction and rapid growth of metal particles should be efficiently avoided, then metal nanostructures could be directly fabricated in aqueous solutions of metal ions [83–85]. Following this line, a surfactants-assisted pathway was developed (Fig. 7a). Duan and co-workers [83] reported that, with the aid of suitable surfactants as metal particles growing inhibitor, refined 3D silver structures were successfully fabricated (Fig. 7b). Through controlling the laser power and the concentration of surfactants, sub-diffraction-limit resolution was achieved. The minimum feature sizes are as high as  $180 \text{ nm}$  for the 3D structures and  $120 \text{ nm}$  for 2D patterns, respectively. In addition, by careful control of the photosensitivity of the metal ion solution, we recently developed a novel 3D metal nanowiring route [85]. Conductive silver nanowires on various nonplanar substrates were achieved by FSLDW (Fig. 7c). An open problem still exists in the field, that is, surface modification of silver nanoparticles for their better mechanical connection towards complicated struc-

tures which generally lead to worse electric conductivity. If this problem is solved, the technology may find greater use in fabrication of plasmonic devices, which has been considered a promising candidate in on-chip optical connection.

### Other routes

Similar to the processing of positive-tone photoresists [46], femtosecond laser induced component removal of bulky solids could also be utilized for 3D nanostructuring. Typical example is femtosecond laser ablation, on which numerous reports could be easily found [86–89], thus we would not reach details on it. Here, we would like to exhibit a novel example of FSLDW induced components removal for graphene micro-nanostructuring. Recently, graphene has attracted enormous attention due to its unique properties, such as high mobility, 2D Dirac fermions, room-temperature quantum Hall effect and high elasticity [90], which make the 2D carbon crystal a promising material for electrical devices. However, despite the solution-processing compatibility, mass-produced graphene oxide suffers from nonconductive nature due to the oxygen defects [91], and therefore, deoxidation is essential before their electrical use. Unlike conventional reduction routes such as high-temperature treatment ( $>1000 \text{ }^\circ\text{C}$ ) and chemical reduction which are not compatible with devices preparation, femtosecond laser was proved capable for efficient reduction and synchronous nanopatterning of graphene oxide [51]. As shown in Fig. 8a, graphene microcircuits were created between two electrodes according to computer programs, giving the integrative feasibility and designability for microdevices. AFM images show that the laser-reduced graphene surface is sunken, caused by the removal of oxygen-containing groups (Fig. 8b and c). Importantly, the reduced graphene microcircuits are conductive and the conductivity is controllable, confirming the effective reduction (Fig. 8d). The direct reduction and patterning of graphene *via* FSLDW might imply an alternative technical route for microelectronic devices and the possibility of part substitution of “graphene plus FSLDW” for “silicon plus lithography”. An immediate work along this line would be circuit writing in controlled ambient of gases so that the conductivity and *p*, *n* type semiconductority could be better controlled.

### Broad applications as a universal tool

The role of FSLDW as a nano-enabler has been established due to its 3D processing capability, the arbitrary designability, and reasonably high spatial resolution. These features make it possible to solve problems encountered in frontiers of diverse scientific fields and industrial applications, which are otherwise not possible. How the technology may impact IC industry from the point of view of microelectronic devices fabrication has been manifested in Figs. 7(c) and 8 and related text. In this session, several more examples in micro-nanomachine, microoptics, and microfluidics have been chosen to further illuminate its broad application as a universal tool.

For micro-nanomachines fabrication, multiple-run electron beam lithography aided with purposely induced

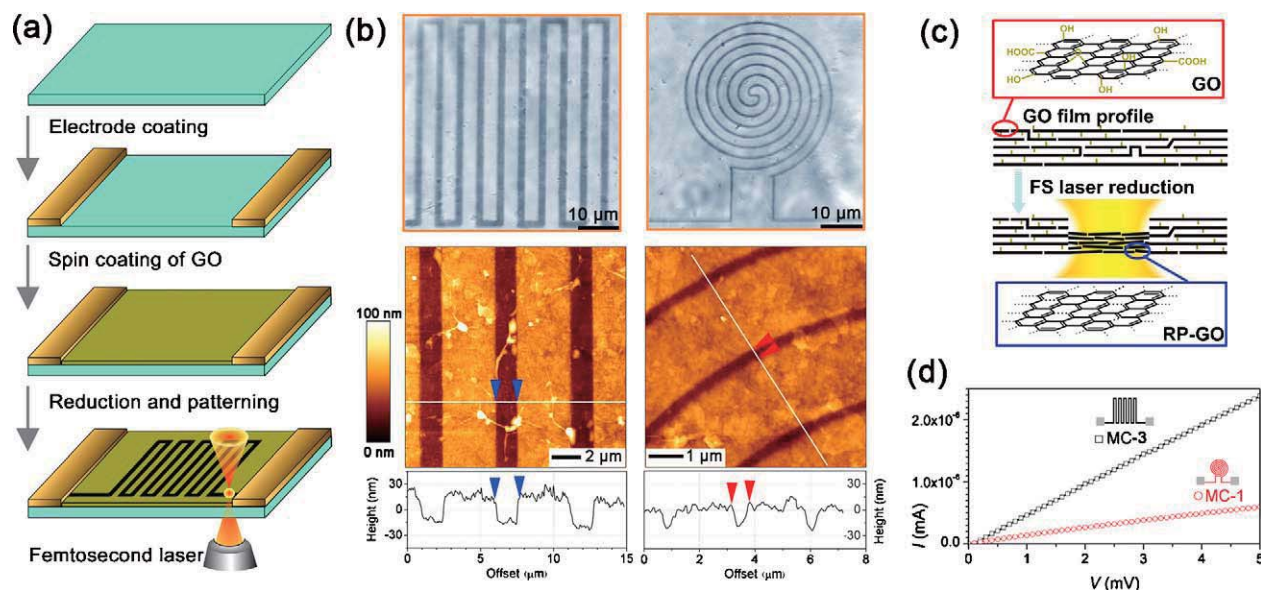


**Figure 8** Femtosecond laser direct writing induced deoxygenation for reducing and patterning graphene oxides. (a) Illustration of preparative procedure; (b) optical microscopy images and AFM results of the graphene patterns; (c) illustration of FsLDW induced deoxygenation and the generation of sunken surface; (d)  $I$ - $V$  curves of the reduced and patterned graphene microcircuits which indicate their conductivities.

Reproduced with permission from [51]. ©2010 Elsevier.

sacrifice layers has been proved a successful technical avenue. However, the manufacturing yield and cost increase versus the structural complexity, and therefore the run number, and the technology is basically applicable to silicon material. FsLDW enables the concept of polymer MEMS, and the fabrication was not complicated by the structural complexity because of its nature one-run depicting from the computer design. Versatile functional materials with their performance comparable with inorganic counterparts or even better may be utilized. For manipulation of these micromachines, ferromagnetic nanoparticles have been doped into photopolymerizable resin after surface modification to reach a status of ferrofluidics, which permits doping percentage as high as 20% in mass [53,54] (Fig. 9a–c). With the mixed material, similar oscillators have been produced, and were freely operated with the stimuli from an external magnetical field, like bending, swinging, and extension (Fig. 9c). An important problem needs solving for practically useful polymer MEMS is the induction of electrical conductivity. Conductive polymers do not seem to be a good solution because of their optical opacity arising from the high absorption to the fabrication lasers, while coating or evaporation does not provide sufficient mechanical adhesion between the metal films and polymer surface. Solution may be found in hybridization of inorganic and organic materials, for example, use of carbon nanotubes.

In the field of microoptics, fabrication of microoptical components with complex surface shapes required by optical functions is a thorny issue since conventional technology such as diamond milling is no more useful at small scale. For example, an ideal microlens possess an aspheric surface profile defined by a high-order lens function, as is not possibly realized by technologies like thermal reflow or soft-lithography. The task can be easily accomplished by computer design followed with FsLDW. Shown in Fig. 3(c)

is actually an ellipsoid aspheric microlens. The root mean square deviation of the measured surface profile from the theoretical design is as small as  $\lambda/40$ , where  $\lambda$  is the fabrication wavelength. Compared with single lenses, even more useful are the microlens arrays, which have readily produced planar close package of triangular, square, and hexagonal edge-cut aspherical lens. These microlens array intrinsically possesses 100% fill ratio [44], meaning that all light passing through the arrays are focused by the lenslets (Fig. 9e). It is worthy to mention the optical resolving power of the lens array, indicated by the lens NA, as high as 0.48, is far higher than those fabricated by other technologies, at the level of 0.1. If the circle diameter of cross-sections along the optical axis of an aspheroid decays exponentially, the lens focus light into a beam instead of a single point. The lens is called axicone, which allows for large focal depth imaging. For example, invariant imaging along 400  $\mu\text{m}$  focal depth for a lens of 100- $\mu\text{m}$  diameter has been attained [45]. In addition to direct surface shape control, it is possible to design the spatial distribution of effective refractive index by tailoring the occupation percentage of dielectrics (e.g., polymers) in matrix (e.g., air). A typical example is the work by Wegner's group on invisible cloak [92]. Based on transformation optics, they designed and directly wrote a diamond lattice PhC structure, on which a region of a bump with gradually varied polymer filling ration beneath is induced. The structure operates as a cloak with a large bandwidth of unpolarized light from 1.4 to 2.7  $\mu\text{m}$  for viewing angle up to 60°. In the above works, the irreplaceable role of FsLDW as an enabling tool for fundamental optical physics and frontier photonic applications has been manifested. The low refractive index, around 1.5, of photopolymers is sometimes a limit for use of the technology in optics. For example, full photonic bandgap is difficult to attain in polymer PhCs no matter what types of lattices are adopted. Doping of high

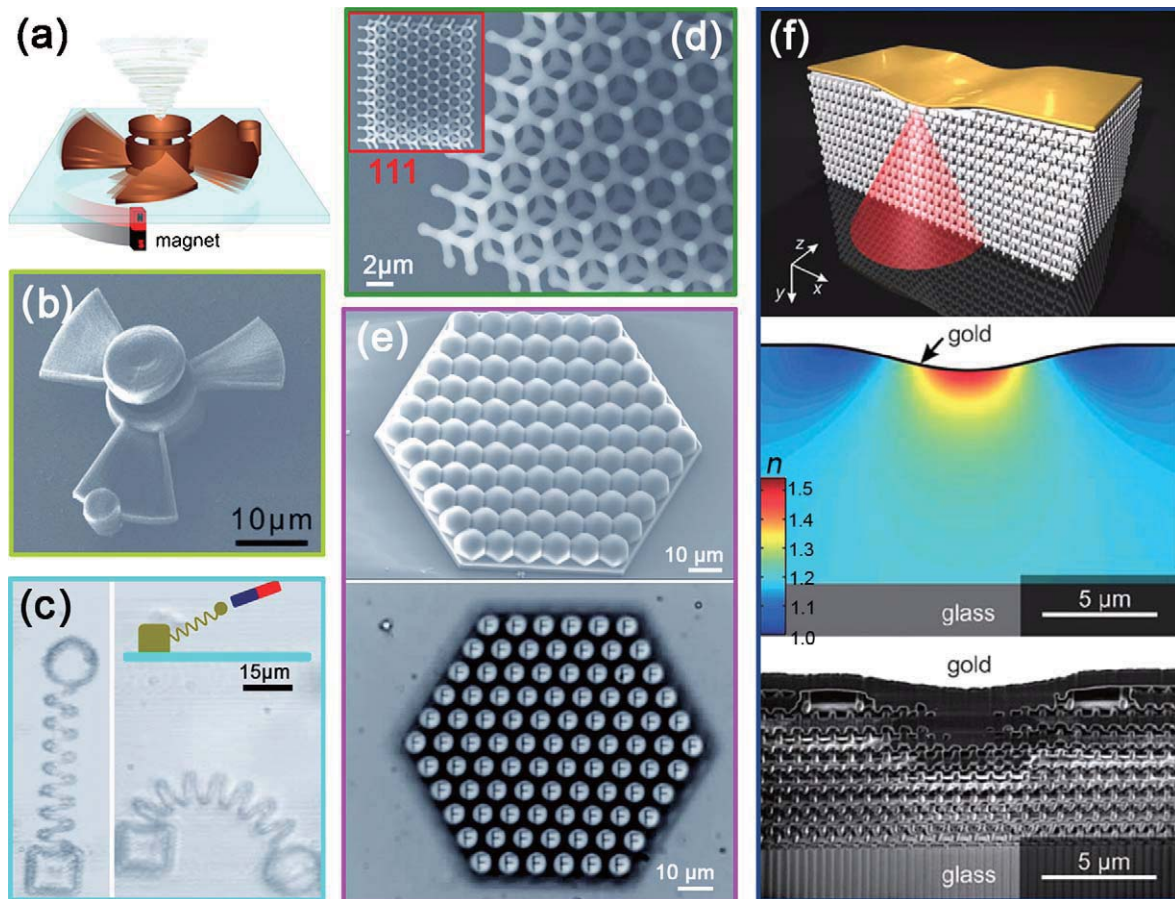


**Figure 9** Examples of the applications of various micro-nanostructures created with FsLDW. (a) schematic illustration of a remotely controllable micro-nanomachines; (b) SEM image of remotely controllable microturbine which is fabricated by FsLDW in photopolymerizable ferrofluids; (c) remote control of magnetic micro-spring; (d) diamond photonic crystals (PhCs) fabricated with FsLDW; (e) SEM images of gapless high-quality microlens arrays (HMLAs, height:  $2.4\ \mu\text{m}$ ), and their arrays of miniaturized “F” images; (f) blueprint of our 3D carpet-cloak structure. The 3D cone of light corresponding to the  $\text{NA} = 0.5$  microscope lens is shown in red (top). Target refractive index ( $n$ ) distributions (middle) and oblique-view electron micrographs of fabricated structures after FIB milling (bottom). Note that the oblique view in the electron micrographs compresses the  $y$ -direction. Reproduced with permission from [43,53,54,92]. ©2010 American Institute of Physics, 2009 Optical Society of America, 2010 Wiley–VCH, 2010 American Association for the Advancement of Science

index components like  $\text{TiO}_2$  [73] provides simple solution to the issue, but the fabrication quality should be further improved.

Application of FsLDW on microfluidic systems is a quite new topic compared with the history of the past two decades, when interests in scaled-down analytical processes with the concept of microfluidics are motivating the rapid progress of “lab-on-a-chip” (LoC) systems [93]. With LoC, biological and chemical assays are being conducted more rapidly, at lower cost and with smaller amount of samples, which strongly stimulate the development of new techniques for the fabrication of microfluidic devices. For example, ultraviolet (UV), e-beam, X-ray lithographies, soft-lithography, and nanoimprint methodologies were successfully used to create planar microfluidic channels. Despite these efforts, up to now, it is still difficult to make refined microfluidic chips with complex 3D topological structures in a designable, flexible, and controllable fashion. These issues are liable to be solved by FsLDW. Wu et al. [56] proposed a nanoshell prototyping method

(Fig. 4d), by which buried channels could be defined with an efficiency improved by orders of magnitude compared with point-by-point TPP exposure. Furthermore, Kumi et al. [94] utilized a novel photoacid generator with high two-photon absorption cross-section in an SU8 resist, which lowered the threshold of photopolymerization and therefore allowed for high-speed scanning exposure. High aspect ratio master structures are therefore attained for creation of reverse microfluidic channels (Fig. 10a). Although templates produced this way are difficultly extended to 3D or more complex structures, the writing speed improvement is an important stage for industrial use of the FsLDW on LoC systems. An even simple use of the technology is embellishment of ready microfluidic channels for advanced functions [95]. Shown in Fig. 10b and c are microsieves and one-way microvalve inside a microchannel. The fabrication of these simple structures, both with vertical arrangement relative to the substrate surface is almost impossible by simple lithography. Experimentally it has been demonstrated that particles of size larger than the pore size cannot pass

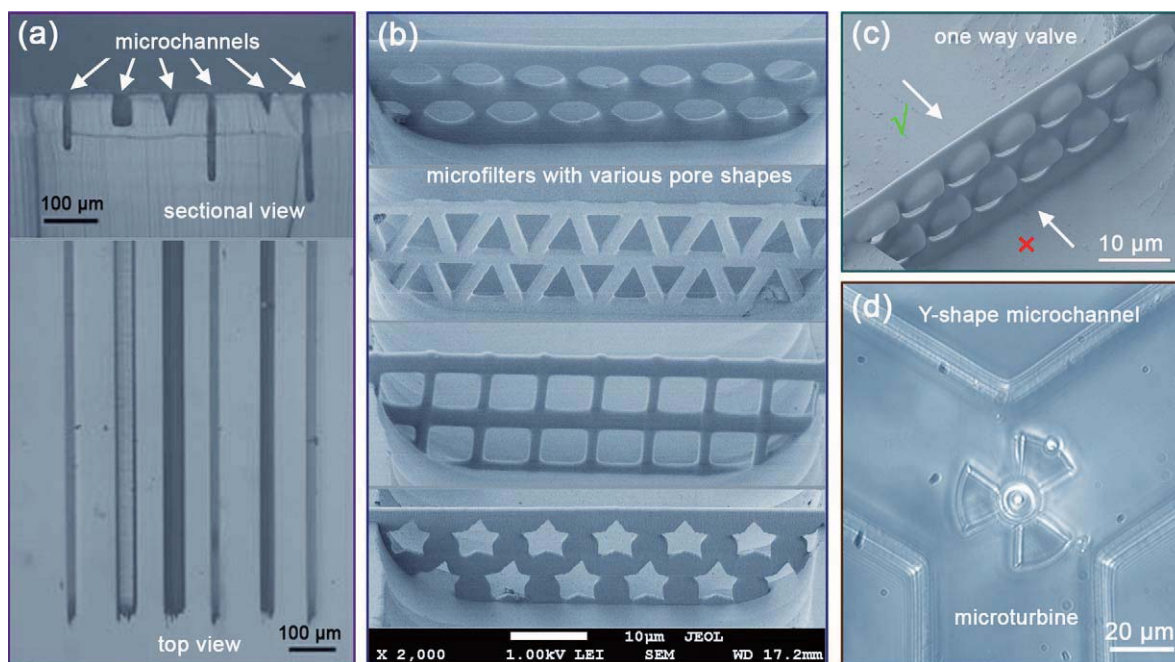


**Figure 10** (a) Optical image of PDMS micro-channels with different cross-sections and heights. Each wall is approximately  $1000\ \mu\text{m}$  long, and the cross-sectional view of the same mold. The scale bars are  $100\ \mu\text{m}$ . (b–d) FsLDW for microfluidic chip functionalization. (b) Microsieves and (c) one-way microvalves were fabricated inside a microchannel for sieving microparticles and control of their flowing direction, respectively; (d) magnetic microturbine fabricated inside a “Y” channel as a mixing microdevice. Reproduced with permission from [94,95]. ©2010 The Royal Society of Chemistry.

through the sieves, as is expected to perform functions like cell sorting. Further use of purposely synthesized materials, more functional parts may be produced. For example, Tian et al synthesized oleic acid stabilized  $\text{Fe}_3\text{O}_4$  nanoparticles *via* high-temperature induced organic phase decomposition of an iron precursor, which was then surface-modified with propoxylated trimethylolpropane triacrylate (PO3-TMPTA, a kind of cross-linker) [96]. The magnetic nanoparticles were then homogeneously doped in acrylate-based photoresist, by which a magnetically controllable microturbine was produced. Such components provide effective alternative means for microfluids mixing. The capability of integrating additional structures in substrates that contain early created devices is unique, which relaxes much the harsh requirement of material and technological compatibility in the fabrication of highly integrated systems. The FsLDW approach may be not best suited for batch production of 2D or simple LoC systems even if the fabrication efficiency is further improved because of the cost consideration, however, a lot is being expected on their use in chips consisting of 3D channels for tissue engineering, and complicated “bio-box” made of optical, electrical and mechanical components.

## Concluding remarks

We briefly review the state of the art of FsLDW technology with a particular emphasis placed on a systematic analysis why fabrication resolution far beyond the optical diffraction limit has been achieved. Three factors, namely optical nonlinearity (the narrowed spatial distribution of equivalent light intensity), chemical nonlinearity (thresholding effect

induced photopolymerization rate out of proportion to the radicals concentration), and material nonlinearity (materials shrinkage due to removal of small molecules escape from polymer network in solvents) are responsible. Smallest standalone voxel (not suspended lines) so far observed is around  $100\ \text{nm}$ . Less volume should be achievable, but it is difficult for them to survive solvent rinsing and SEM observation under electron beam. The accuracy of shape prototyping is found much better than the scale of voxel itself because voxels can arbitrarily overlap with each other, as permits definition of patterns of any shape and volume larger than a voxel. As for the surface, smoothness of several nanometers has been achieved due to the filling of liquid or partly polymerized resins to the intersecting corners of voxels and an ensuing self-smoothing effect caused by surface tension in the course of resin rinsing.

Many photochemical effects may be utilized for FsLDW towards micro-nanodevice fabrication only if sufficient contrast of material property is formed between the femtosecond laser irradiated volumes and nonirradiated background. In case of photopolymerization of negative-tone resins, the irradiated portion (voxels) is solidified; for photoisomerization of DPO-PPV, laser-generated transform molecules become insoluble; and in photoreduction of metal ions, newly reduced metal atoms are insoluble, to be attached to early produced framework. Different from the above three cases, positive-tone resins undergo photolysis of macromolecules in the irradiated volume, where solubility is rendered and is to be removed for shape prototyping. This feature makes it a good choice for fabrication of structures with high-density buried channels or holes. The graphene oxide film is not necessarily removed after graphene cir-

cuits are drawn by FsLDW because it provides functions of mechanical supporting and electrical isolation.

FsLDW has been considered as a universal nanofabrication tool not only because the useful material species is unlimited, but also due to the manufactured devices may bring revolutionary changes of micro-nanodevice fabrication technology in diversified scientific and industrial fields. For example, it enables high precision fabrication of aspheric microlenses and micro-axicon lenses and their array for high-quality miniaturized imaging system, remotely controllable micromachines such as micro-oscillator and microturbines, essential components like microsieves and one-way valves, as well as in the near future, 3D microfluidic devices for microanalysis. Even exciting is the prospect of graphene circuits as a novel concept of microelectronic devices. However, an intrinsic shortcoming of the FsLDW associated with the point-by-point writing strategy is the relatively low fabrication efficiency as compared with the bottom-up methods, and the high fabrication quality has not yet achieved in all needed materials species so far. As a novel field, there are still many open problems as we pointed out. However, we believe the continuous efforts on exploration of novel materials, optical technologies and photochemical mechanisms should bring more exciting future of the FsLDW technology.

## Acknowledgement

The authors acknowledge the financial support from NSFC under grant Nos. 61008014, 90923037, 60778004, 60978048, and 60525412.

## References

- [1] S.E.A. Gratton, S.S. Williams, A.E. Napier, P.D. Pohlhaus, Z.L. Zhou, K.B. Wiles, et al., *Acc. Chem. Res.* 41 (2008) 1685.
- [2] B.D. Gates, Q.B. Xu, M. Stewart, D. Ryan, C. Grant Willson, G.M. Whitesides, *Chem. Rev.* 105 (2005) 1171.
- [3] K. Ariga, J.P. Hill, Q. Ji, *Phys. Chem. Chem. Phys.* 9 (2007) 2319.
- [4] T. Shimizu, *Polym. J.* 35 (2003) 1.
- [5] M. Shimomura, T. Sawadaishi, *Curr. Opin. Colloid. In.* 6 (2001) 11.
- [6] N. Wu, W.B. Russel, *Nano Today* 4 (2009) 180.
- [7] O. Hayden, R. Agarwal, W. Lu, *Nano Today* 3 (2008) 12.
- [8] Y.F. Li, J.H. Zhang, B. Yang, *Nano Today* 5 (2010) 117.
- [9] S. Kitayaporn, J.H. Hoo, K.F. Bohringer, F. Baneyx, D.T. Schwartz, *Nanotechnology* 21 (2010) 1.
- [10] Y.D. Yan, Z.J. Hu, X.S. Zhao, T. Sun, S. Dong, X.D. Li, *Small* 6 (2010) 724.
- [11] S.Y. Chen, J.G. Bomer, W.G. van der Wiel, E.T. Carlen, A. van der Berg, *ACS Nano* 3 (2009) 3485.
- [12] J.Y. Cheng, C.A. Ross, H.I. Smith, E.L. Thomas, *Adv. Mater.* 18 (2006) 2505.
- [13] D.P. Sanders, *Chem. Rev.* 110 (2010) 321.
- [14] F. Cerrina, *J. Phys. D: Appl. Phys.* 33 (2000) 103.
- [15] A.E. Grigorescu, C.W. Hagen, *Nanotechnology* 20 (2009) 1.
- [16] S. Kramer, R.R. Fuieler, C.B. Gorman, *Chem. Rev.* 103 (2003) 4367.
- [17] S.M. Yang, S.G. Jang, D.G. Choi, S. Kim, H.K. Yu, *Small* 2 (2006) 458.
- [18] L.J. Guo, *Adv. Mater.* 19 (2007) 495.
- [19] V.N. Truskett, M.P.C. Watts, *Trends Biotechnol.* 24 (2006) 312.
- [20] L.J. Guo, *J. Phys. D: Appl. Phys.* 37 (2004) 123.
- [21] R.R. Gattass, E. Mazur, *Nat. Photonics* 2 (2008) 219.
- [22] L.J. Li, J.T. Fourkas, *Mater. Today* 10 (2007) 30.
- [23] B.H. Cumpston, S.P. Ananthavel, S. Barlow, D.L. Dyer, J.E. Ehrlich, L.L. Erskine, et al., *Nature* 398 (1999) 51.
- [24] L.J. Li, R.R. Gattass, E. Gershgoren, H. Hwang, J.T. Fourkas, *Science* 324 (2009) 910.
- [25] M. Malinauskas, A. Zukauskas, G. Bickaускаite, R. Gadonas, S. Juodkazis, *Opt. Express* 18 (2010) 10209.
- [26] S.H. Park, D.Y. Yang, K.S. Lee, *Laser Photonics Rev.* 3 (2009) 1.
- [27] K.S. Lee, R.H. Kim, D.Y. Yang, S.H. Park, *Prog. Polym. Sci.* 33 (2008) 631.
- [28] K.S. Lee, D.Y. Yang, S.H. Park, R.H. Kim, *Polym. Adv. Technol.* 17 (2006) 72.
- [29] T.C. Chong, M.H. Hong, L.P. Shi, *Laser Photonics Rev.* 4 (2010) 123.
- [30] S. Kawata, H.B. Sun, T. Tanaka, K. Takada, *Nature* 412 (2001) 697.
- [31] H.B. Sun, S. Kawata, *Adv. Polym. Sci.* 170 (2004) 169.
- [32] T. Tanaka, H.B. Sun, S. Kawata, *Appl. Phys. Lett.* 80 (2002) 312.
- [33] P. Zijlstra, J.W.M. Chou, M. Gu, *Nature* 459 (2009) 410.
- [34] Z.B. Sun, X.Z. Dong, W.Q. Chen, S. Nakanishi, X.M. Duan, S. Kawata, *Adv. Mater.* 20 (2008) 914.
- [35] H.B. Sun, K. Takada, M.S. Kim, K.S. Lee, S. Kawata, *Appl. Phys. Lett.* 83 (2003) 1104.
- [36] H.B. Sun, T. Tanaka, S. Kawata, *Appl. Phys. Lett.* 80 (2002) 3673.
- [37] H.B. Sun, S. Kawata, *J. Lightwave Technol.* 21 (2003) 624.
- [38] H.B. Sun, M. Maeda, K. Takada, J.W.M. Chon, M. Gu, S. Kawata, *Appl. Phys. Lett.* 83 (2003) 819.
- [39] J. Morikawa, A. Orié, T. Hashimoto, S. Juodkazis, *Appl. Phys. A* 98 (2010) 551.
- [40] K. Takada, K. Kaneko, Y.D. Li, S. Kawata, Q.D. Chen, H.B. Sun, *Appl. Phys. Lett.* 92 (2008) 041902–41911.
- [41] K. Takada, D. Wu, Q.D. Chen, S. Shoji, H. Xia, S. Kawata, et al., *Opt. Lett.* 34 (2009) 566.
- [42] D.F. Tan, Y. Li, F.J. Qi, H. Yang, Q.H. Gong, X.Z. Dong, et al., *Appl. Phys. Lett.* 90 (2007) 071106–71111.
- [43] D. Wu, S.Z. Wu, L.G. Niu, Q.D. Chen, R. Wang, et al., *Appl. Phys. Lett.* 97 (2010) 031109.
- [44] D. Wu, Q.D. Chen, L.G. Niu, J. Jiao, H. Xia, J.F. Song, et al., *IEEE Photonic Technol. Lett.* 21 (2009) 1535.
- [45] X.F. Lin, Q.D. Chen, L.G. Niu, T. Jiang, W.Q. Wang, H.B. Sun, *IEEE J. Lightwave Technol.* 28 (2010) 1256.
- [46] W.H. Zhou, S.M. Kuebler, K.L. Braun, T.Y. Yu, J.K. Cammack, C.K. Ober, et al., *Science* 296 (2002) 1106.
- [47] T.Y. Yu, C.K. Ober, S.M. Kuebler, W.H. Zhou, S.R. Marder, J.W. Perry, *Adv. Mater.* 15 (2003) 517.
- [48] Y. Zhou, M.H. Hong, J.Y.H. Fuh, L. Lu, B.S. Lukyanchuk, Z.B. Wang, et al., *Appl. Phys. Lett.* 88 (2006) 023110–23111.
- [49] M. Watanabe, S. Juodkazis, H.B. Sun, S. Matsuo, H. Misawa, M. Miwa, et al., *Appl. Phys. Lett.* 74 (1999) 3957.
- [50] A. Zoubir, M. Richardson, C. Rivero, A. Schulte, C. Lopez, K. Richardson, et al., *Opt. Lett.* 29 (2004) 748.
- [51] Y.L. Zhang, L. Guo, S. Wei, Y.Y. He, H. Xia, Q.D. Chen, et al., *Nano Today* 5 (2010) 15.
- [52] H.B. Sun, T. Tanaka, K. Takada, S. Kawata, *Appl. Phys. Lett.* 79 (2001) 1411.
- [53] J. Wang, H. Xia, B.B. Xu, L.G. Niu, D. Wu, Q.D. Chen, *Opt. Lett.* 34 (2009) 581.
- [54] H. Xia, J. Wang, Y. Tian, Q.D. Chen, X.B. Du, Y.L. Zhang, et al., *Adv. Mater.* 22 (2010) 3204.
- [55] D.Y. Yang, S.H. Park, T.W. Lim, H.J. Kong, S.W. Yi, H.K. Yang, et al., *Appl. Phys. Lett.* 90 (2007) 013113–13121.
- [56] D. Wu, Q.D. Chen, L.G. Niu, J.N. Wang, J. Wang, R. Wang, et al., *Lab. Chip* 9 (2009) 2391.
- [57] H.B. Sun, T. Kawakami, Y. Xu, J.Y. Ye, S. Matuso, H. Misawa, et al., *Opt. Lett.* 25 (2000) 1110.

- [58] K. Kaneko, H.B. Sun, X.M. Duan, S. Kawata, *Appl. Phys. Lett.* 83 (2003) 2091.
- [59] H.B. Sun, T. Suwa, K. Takada, R.P. Zaccaria, M.S. Kim, K.S. Lee, et al., *Appl. Phys. Lett.* 85 (2004) 3708.
- [60] J.I. Kato, N. Takeyasu, Y. Adachi, H.B. Sun, S. Kawata, *Appl. Phys. Lett.* 86 (2005) 044102–44111.
- [61] X.Z. Dong, Z.S. Zhao, X.M. Duan, *Appl. Phys. Lett.* 91 (2007) 124103–124111.
- [62] M. Albota, D. Beljonne, J.L. Bredas, J.E. Ehrlich, J.Y. Fu, A.A. Heikal, et al., *Science* 281 (1998) 1653.
- [63] K.D. Belfield, K.J. Schafer, W.J. Mourad, *J. Org. Chem.* 65 (2000) 4475.
- [64] J. Jortner, M. Ratner (Eds.), *Molecular Electronics*, Blackwell Science, 1997.
- [65] K.D. Belfield, D.J. Hagan, E.W. Van Stryland, K.J. Schafer, R.A. Negres, *Org. Lett.* 1 (1999) 1575.
- [66] S.J. Chung, M. Bumi, V. Alain, S. Barlow, J.W. Perry, S.R. Marder, *J. Am. Chem. Soc.* 127 (2005) 10844.
- [67] A.M. Kloxin, K.S. Anseth, *Nature* 7 (2008) 454.
- [68] B. Kaehr, J.B. Shear, *Proc. Natl. Acad. Sci. U.S.A.* 105 (2008) 8850.
- [69] B. Kaehr, J.B. Shear, *J. Am. Chem. Soc.* 129 (2007) 1904.
- [70] S.K. Seidlits, C.E. Schmidt, J.B. Shear, *Adv. Funct. Mater.* 19 (2009) 3543.
- [71] G. Velze-Casquillas, M.L. Berre, M. Piel, P.T. Tran, *Nano Today* 5 (2010) 28.
- [72] H. Xia, W.Y. Zhang, F.F. Wang, D. Wu, X.W. Liu, L. Chen, et al., *Appl. Phys. Lett.* 95 (2009) 083118–83121.
- [73] S. Passinger, M.S.M. Saifullah, C. Reinhardt, K.R.V. Subramanian, B.N. Chichkov, M.E. Welland, *Adv. Mater.* 19 (2007) 1218.
- [74] L. Guo, H. Xia, H.T. Fan, Y.L. Zhang, Q.D. Chen, T. Zhang, et al., *Opt. Lett.* 35 (2010) 1695.
- [75] R. Houbertz, L. Frohlich, M. Popall, U. Streppel, P. Dannberg, A. Brauer, et al., *Adv. Eng. Mater.* 5 (2003) 551.
- [76] K. Awazu, M. Fujimaki, C. Rockstuhl, J. Tominaga, H. Murakami, Y. Ohki, et al., *J. Am. Chem. Soc.* 130 (2008) 1676.
- [77] A. Ishikawa, T. Tanaka, S. Kawata, *Phys. Rev. Lett.* 95 (2005) 237401.
- [78] Y.L. Wu, Y.N. Li, B.S. Ong, *J. Am. Chem. Soc.* 128 (2006) 4202.
- [79] J.R. Lakowicz, *Plasmonics* 1 (2006) 5.
- [80] K. Kaneko, H.B. Sun, X.M. Duan, S. Kawata, *Appl. Phys. Lett.* 83 (2003) 1426.
- [81] S. Maruo, T. Saeki, *Opt. Express* 16 (2008) 1174.
- [82] L. Vurth, P. Baldeck, O. Stephan, G. Vitrant, *Appl. Phys. Lett.* 92 (2008) 171103–171111.
- [83] Y.Y. Cao, N. Takeyasu, T. Tanaka, X.M. Duan, S. Kawata, *Small* 5 (2009) 1144.
- [84] Y.Y. Cao, X.Z. Dong, N. Takeyasu, T. Tanaka, Z.S. Zhao, X.M. Duan, S. Kawata, *Appl. Phys. A* 96 (2009) 453.
- [85] B.B. Xu, H. Xia, L.G. Niu, Y.L. Zhang, K. Sun, Q.D. Chen, et al., *Small* 6 (2010) 1762.
- [86] Y. Lin, M.H. Hong, T.C. Chong, C.S. Lim, G.X. Chen, L.S. Tan, et al., *Appl. Phys. Lett.* 89 (2006) 041108–41111.
- [87] Y. Lin, M.H. Hong, W.J. Wang, Y.Z. Law, T.C. Chong, *Appl. Phys. A* 80 (2005) 461.
- [88] S.M. Huang, M.H. Hong, B.S. Lukyanchuk, T.C. Chong, *Appl. Phys. Lett.* 82 (2003) 4809.
- [89] M. Watanabe, S. Juodkazis, H.B. Sun, S. Matsuo, H. Misawa, *Appl. Phys. Lett.* 77 (2000) 13.
- [90] A.K. Geim, K.S. Novoselov, *Nat. Mater.* 6 (2007) 183.
- [91] G. Eda, G. Fanchini, M. Chhowalla, *Nat. Nanotechnol.* 3 (2008) 270.
- [92] T. Ergin, N. Stenger, P. Brenner, J.B. Pendry, M. Wegener, *Science* 328 (2010) 337.
- [93] M.S. Lord, M. Foss, F. Besenbacher, *Nano Today* 5 (2010) 66.
- [94] G. Kumi, C.O. Yanez, K.D. Belfield, J.T. Fourkas, *Lab. Chip* 10 (2010) 1057.

[95] J. Wang, Y. He, H. Xia, L.G. Niu, R. Zhang, Q.D. Chen, et al., *Lab. Chip* 10 (2010) 1993.

[96] Y. Tian, Y.L. Zhang, J.F. Ku, Y. He, B.B. Xu, Q.D. Chen, et al., *Lab. Chip* 10 (2010) 2902.



**Dr. Yong-Lai Zhang** was born in Liaoning, China in 1981. He received his B.S. in Chemistry (2004) and Ph.D. in Inorganic Chemistry (2009) from Jilin University. In 2008, he had worked in Fritz-Haber-Institut of the Max-Planck-Gesellschaft on the TEM characterization. After received his Ph.D, he joined in Prof. H.-B. Sun's group in the State Key Laboratory on Integrated Optoelectronics, College of Electronic Science and Engineering, Jilin University. His current

research is focused on the fabrication of polymeric and inorganic micro-nanostructures via femtosecond laser direct writing for the applications in micromachines, microdevices and lab-on-a-chip system. He is also interested in graphene-based materials and devices.



**Associate Prof. Qi-Dai Chen** was born in 1976 in Shandong, China. He received his B.S. in Physics (1998) from University of Science and Technology of China. In 2004, he received his Ph.D. from Institute of Physics, Chinese Academy of Sciences. After postdoctoral work at the Osaka City University at Japan, he joined the faculty at Jilin University in 2006. His main research is focused on laser micro-nanofabrication and ultrafast spectroscopy.



**Associate Prof. Hong Xia** was born in Shuangcheng, China in 1980. She received her B.S. and Ph.D. degree in Chemistry from Jilin University in 2001 and 2006. She joined the faculty at Jilin University in 2006, where she is now an associate professor of photo-electronics. Her research is focused on micro-nanofabrication by laser based on functional resins and polymers.



**Prof. Hong-Bo Sun** received the B.S. and the Ph.D. degrees in electronics from Jilin University in 1992 and 1996, respectively. He worked as a postdoctoral researcher in University of Tokushima, Japan, from 1996 to 2000, and then as an assistant professor in the Department of Applied Physics, Osaka University. He became a project leader under PRESTO (Precursory Research for Embryonic Science and Technology, Japan) program in 2001. He

was awarded by Optical Science and Technology Society for his contribution to the technology of femtosecond laser initiated nanofabrication in 2002, and won Outstanding Young Scientist Award issued by the minister of MEXT (Ministry of Education, Culture, ports, Science & Technology, Japan) in 2006. In 2005, he was promoted as a full professor (Changjiang Scholar) at Jilin University, China. He won National Natural Science Funds for Distinguished Young Scholar, China, in 2005, and his team was supported by PCSIRT (Program for Changjiang Scholars and Innovative Research Team at University, China) in 2007. Prof. Sun's research has been focused on laser micro-nanofabrication in the past 10 years, particularly in exploring novel laser technologies including direct writing and holographic lithography, as well as their applications on microoptics, micromachines, microfluids, and microsensors.